Available online at www.sciencedirect.com
ScienceDirect
Polymer 48 (2007) 7653–7659
polymer
www.elsevier.com/locate/polymer

An investigation on the molecular mobility through the glass transition of chlorinated butyl rubber

Jinrong Wu [a], Guangsu Huang [a,*], Qiying Pan [a], Jing Zheng [a], Yuchan Zhu [b], Bo Wang [b]

[a] College of Polymer Science and Engineering, State Key Laboratory of Polymer Material Engineering, Sichuan University, Chengdu 610065, China
[b] Department of physics, Wuhan University, Wuhan 430072, China

Received 31 July 2007; received in revised form 17 October 2007; accepted 4 November 2007
Available online 7 November 2007

Abstract

In this paper, dynamic mechanical analysis (DMA), dielectric spectroscopy (DS) and positron annihilation lifetime spectroscopy (PALS) were used to study chlorinated butyl rubber (CIIR), in order to shed light on its unique relaxation behaviors. The dynamic mechanical loss tangent of CIIR reveals an asymmetrical broad structure with a maximum peak on the high-temperature side and a shoulder peak on the low-temperature side. DS clarifies that the shoulder peak, which exactly corresponds to the ε'' peak, is the α process originating from the local segmental motion. While the maximum peak is assigned to the slow process arising from the motion of longer chain segments. The slow process exhibits stronger frequency dependence than the α process. The PALS analysis also shows the two processes; moreover, it suggests that CIIR exhibits very effective chain packing. It is due to the effective chain packing that the motion of longer chain segments is retarded and separates from the local segmental motion in time scale. This effect is another reason for the two-peak structure of CIIR, besides the low intermolecular co-operativity.

Keywords: Chlorinated butyl rubber; α Process; Slow process

1. Introduction

In the past decades, the proper nature of molecular mobility near the glass transition of polymers always remains as a hot topic of controversy in the condensed matter physics. Polyisobutylene (PIB), probably the most strong polymer glass-forming liquid, exhibits many distinct relaxation behaviors, which were documented in detail by Plazek and co-workers in one of their papers [1]. Polymers generally exhibit a single maximum in their tan δ (denoting the dynamic mechanical loss tangent if not specially pointed out) versus either frequency or temperature curve, however, as first discovered by Fitzgerald et al. [2], tan δ of PIB reveals an asymmetrical broad peak structure with a maximum peak on the low-frequency (or high-temperature) side and an additional shoulder peak on the other side. Such a phenomenon can also be found in the derivatives of PIB, including butyl rubber (IIR), chlorinated butyl rubber (CIIR) and brominated butyl rubber (BIIR) [3,4]. The two peaks of these polymers are likely related to two relaxation mechanisms, which have inspired a number of works. Sanders and Ferry [5] assigned the maximum peak to the slow relaxation process, and ascribed it to the rearrangement of untrapped entanglements. The process was then designated as liquid–liquid transition by Boyer [6], who argued that the liquid–liquid transition was a transformation from one liquid state to another and arose from the collapse of localized short-range order or the onset of motion of entire polymer chains. Plazek and co-workers [1] identified the maximum peak with Rouse modes, which are known to dominate the viscoelastic response in the glass–rubber transition region and contain in the order of 50 or more backbone bonds, while the shoulder peak with sub-Rouse modes. The sub-Rouse modes they claimed are larger than the couple of conformers involved in local segmental relaxation, while contain fewer chain units than the shortest Gaussian submolecules described by the Rouse model. So the sub-Rouse modes may involve in the order of 10 backbone

* Corresponding author. Tel.: +86 28 85463433; fax: +86 28 85405402.
E-mail address: polymer410@sohu.com (G. Huang).

0032-3861/$ - see front matter © 2007 Elsevier Ltd. All rights reserved.
doi:10.1016/j.polymer.2007.11.006

bonds. Stantangelo et al. [7] pointed out that PIB exhibits weak intermolecular coupling of segmental relaxation due to its smooth, symmetric and flexible structure, which allows the segmental relaxation to occur sufficiently fast. As a result, the segmental relaxation, the sub-Rouse modes and the Rouse modes can be resolved in time, which inhomogeneously broadens the viscoelastic spectrum. Therefore, according to the above discussion, scientists havenot reached an agreement on the definite nature of molecular mobility through the glass transition of PIB and its derivatives.

There are still several works studying the relaxation behaviors of PIB and its derivatives by using dynamic mechanical analysis (DMA) or dielectric spectroscopy (DS) or positron annihilation lifetime spectroscopy (PALS), but none combined the three methods which are powerful in studying relaxation behaviors of polymers to elucidate the previously mention phenomenon [8–12]. In the present study, DMA, DS and PALS were used to study the relaxation behaviors of chlorinated butyl rubber (CIIR), which is a chlorinated copolymer of isobutylene and isoprene (usually 1–2 mol%). The reason why CIIR is chosen to be studied was based on the fact that CIIR is more widely used due to easy vulcanization; furthermore, after chlorination CIIR is dielectrically active compared with the dielectrically inactive PIB, which facilitates the dielectric measurement.

2. Experimental

CIIR (EXXON 1068) with a chlorination concentration of 1.1–1.3 wt% was supplied by Exxon Co. The number average molecular weight of CIIR was determined to be 1.354×10^5 g/mol with a molecular weight distribution of 2.13 by a gel permeation chromatography (GPC, AGILENT-1100) in tetrahydrofuran at 25 °C. Lightly cured CIIR was vulcanized at 160 °C for 20 min with 3 wt% phenolic resin 201 (PR 201), 2 wt% ZnO and 1 wt% stearic acid, while cured CIIR with different crosslinking densities was vulcanized under the same conditions with 5 wt% or 20 wt% PR 201, 5 wt% ZnO and 1 wt% stearic acid.

Dynamic mechanical analysis was carried out on Q800 (TA instruments) by using a mode of dual cantilever clamp and a testing method of temperature step-frequency sweep with each temperature step of 4–6 °C and frequency range from 0.1 Hz to 30 Hz. The sample dimensions were 20 mm long, 12 mm wide and 3 mm thick.

Dielectric measurement was performed on a Novocontrol GmbH Alpha dielectric spectrometer. During the measurement the sample was contained between two parallel plates (diameter 10-mm, gap 1 mm). Temperature was controlled using a nitrogen-gas cryostat with temperature stability better than 0.1 K.

For the measurement of positron annihilation lifetime spectra, a 30 μCi ^{22}Na positron source sealed between two sheets of nickel foil (1 mg/cm^2) was sandwiched between two pieces of the samples and mounted to a cooling head of liquid-nitrogen cryostat with temperature stability better than 0.5 K. Positron lifetime spectra were measured using a conventional fast–fast coincidence spectrometer. The time resolution of the system was found to be a sum of two Gaussians with (fwhm)1 = 280 ps (90%) and (fwhm) = 320 ps (10%). Each spectrum contained approximately 10^6 counts for PATFIT [13], by which all of the measured positron lifetime spectra were resolved into three components after the background and positron source correction was subtracted. The shortest lifetime ($\tau_1 \approx 0.12$ ns) is the lifetime of singlet-positronium (*p*-Ps) and the intermediate lifetime ($\tau_2 \approx 0.40$ ns) is the lifetime of the positron. The longest lifetime ($\tau_3 \approx 1$–3 ns) is due to the *ortho*-positronium (*o*-Ps) pick-off annihilation in the free-volume holes in amorphous phase. Because only the *o*-Ps component is significantly sensitive to the change in the microstructure of the amorphous region, in the present study, we employ the results of *o*-Ps lifetime to obtain the mean free-volume parameters.

3. Results and discussion

Dynamic mechanical spectra of uncured and lightly cured CIIRs are shown in Fig. 1. Unlike other amorphous polymers whose loss peak, generally about 30 K wide, is located near the glass transition region, the dynamic mechanical loss

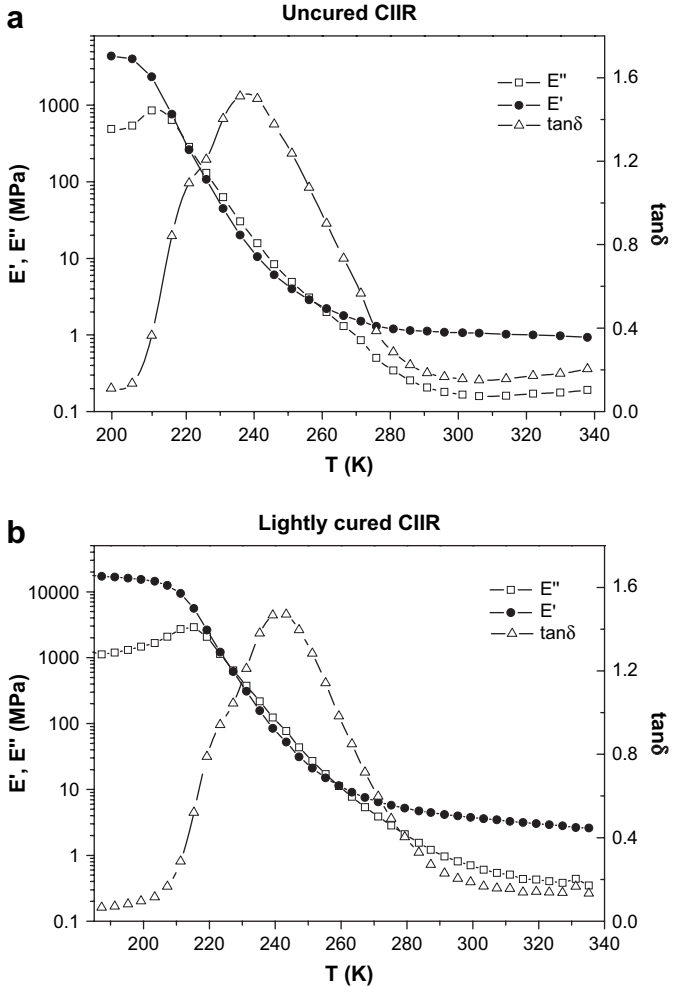

Fig. 1. Dynamic mechanical spectra of uncured and lightly cured CIIR at 1 Hz.

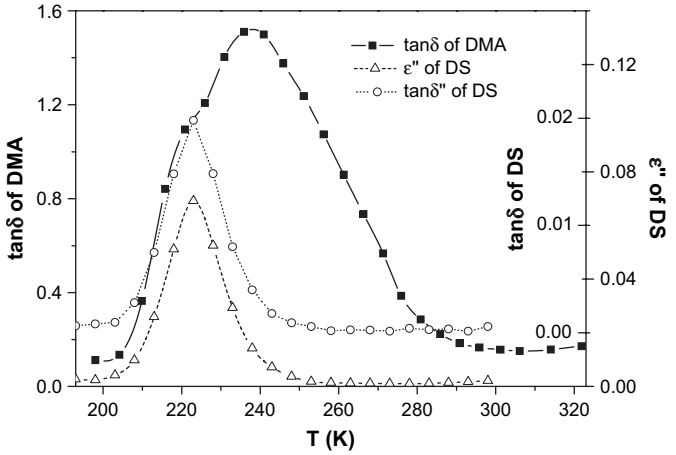

Fig. 2. Dynamic and dielectric loss spectra of uncured CIIR at 1 Hz.

peak of CIIR covering a temperature range from 213 K to 293 K shows an asymmetrical broad structure with a maximum peak at 238 K for uncured CIIR and 241 K for lightly cured CIIR. Additionally, a shoulder peak around 220 K for uncured CIIR and 223 K for lightly cured CIIR can be clearly discerned. Such a phenomenon is the same as PIB, as can be seen in the work of Ferry et al. [2,5] and Plazek et al. [1]. Evidently, there are two relaxation mechanisms responsible for the two peaks.

Fig. 2 presents a comparison between the temperature dependence of tan δ of DMA and that of ε'' and tan δ' (a prime is added in order to distinguish from that of dynamic mechanical analysis) of DS for uncured. Vast difference is self-evident between the two different testing methods. The ε'' peak is almost the same as the tan δ' peak, while both exactly correspond to the shoulder peak of tan δ of dynamic mechanical measurement. It is known that the dielectric measurement detects the fluctuation of dipoles. According to Stockmayer's work [14], the dipoles of polymer chains can be classified into three types, and thereafter this classification is widely used in the dielectric studies [15–18]. The type-A dipoles on the chain backbone have dipole moments paralleling to the chain contour, they reflect the slow dielectric response of the main chain. The type-B dipoles are attached to the chain backbone, and their dipole moments are perpendicular to the chain contour. For chains having type-B dipoles, dielectric measurement provides information on the local segmental motion of their backbone. The local segmental motion, giving rise to the α process and determining the glass transition temperature (T_g), usually involves correlated local motion of only a few backbone bonds. The type-C dipoles are attached to the side chain groups and indicate the motion of side chain groups. Evidently, molecular chains of CIIR are type-B chains, because the chlorine atoms are directly attached to the chain backbone. Therefore, the ε'' and tan δ' peaks of dielectric spectrum can be designated as the α process. On the other hand, segments of all lengths ranging from local segments to long chain segments are expected to contribute to the relaxation of stress and hence be reflected in the dynamic mechanical spectrum. If we regard the broad tan δ peak as the transition region which involves motions of all length-scale segments, the low-temperature shoulder peak, which exactly corresponds to the ε'' and tan δ' peaks of dielectric spectrum, should be designated as the local segmental motion. Since longer chain segments are expected to move at higher temperature or lower frequency and cannot be reflected in dielectric spectrum, the maximum peak should be attributed to the motion of longer chain segments. Because part of Boyer's works about the liquid–liquid transition is discredited [19–23], we just phenomenally name the maximum peak as the slow process in the present work, unlike our previous paper [24].

Fig. 3 exhibits the temperature dependence of tan δ with increasing frequency for uncured and lightly cured CIIRs. It can be observed that the two processes contributing to the two peaks have different frequency shift factors. The slow process responsible for the maximum peak exhibits a stronger frequency dependence than the α process of the shoulder peak. For example, as the frequency varies from 10 Hz to 1 Hz for uncured CIIR, the shoulder peak shifts from about 228 K to 220 K with a interval of 8 K, which is close to the common

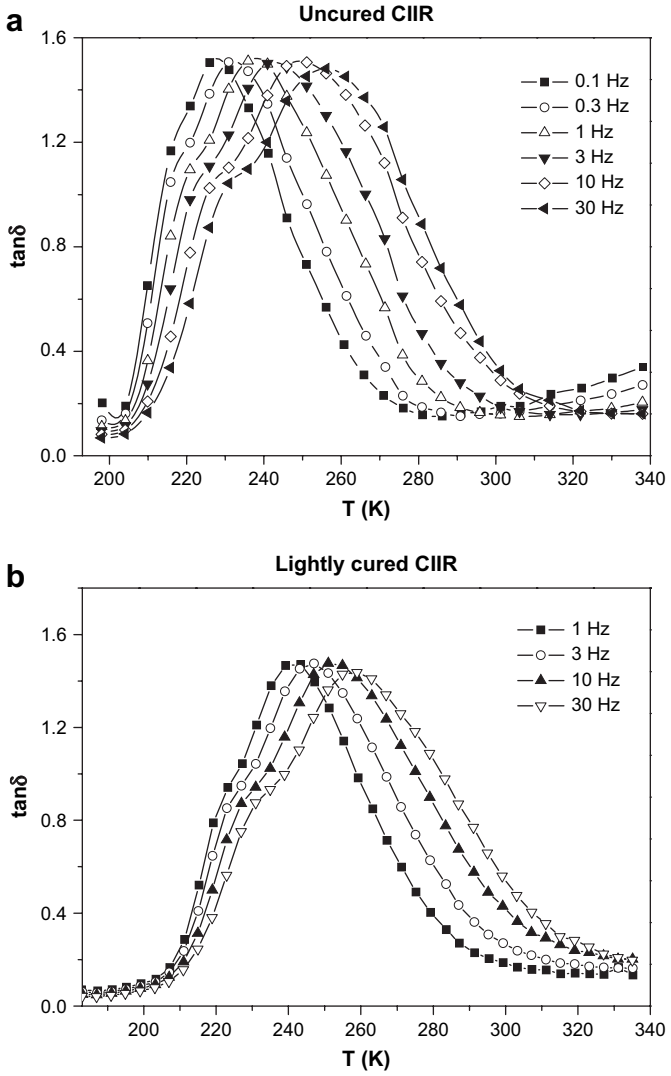

Fig. 3. Frequency dependence of tan δ with increasing temperature of uncured and lightly cured CIIR.

shift interval of 7 K of T_g when the frequency increases/decreases a decade times; however, the maximum peak shifts from 250 K to 238 K with a larger interval of 12 K. So the maximum peak moves to lower temperature faster than the shoulder peak with decreasing frequency. As a result, the whole loss peak become narrower and narrower, and the shoulder peak is almost superposed by the maximum one at low frequencies due to the encroachment of the slow process toward the α process. On the contrary, as the frequency increases, the shoulder peak and the maximum one can be more and more clearly discerned from each other. The phenomenon means that the maximum peak is more sensitive to frequency. Since longer mobile units are more sensitive to the frequency, the longer chain segments of the slow process have more backbone bonds than the local segments of the α process. As illustrated in Fig. 4, it can be seen that vulcanization does not completely suppress the slow process but rather lightly reduces its intensity and shifts it to higher temperature, thereby, the longer chain segments are shorter than the chain segments between two neighboring crosslinking points, which can be roughly estimated from the number average molecular weight to be about 250 backbone bonds on the assumption that isoprene monomers are homogeneously dispersed in the molecular chains and completely react with crosslinking agent. Thus, the longer chain segments may involve from decades to two or three hundreds of backbone bonds.

Using the time–temperature superposition (TTS) principle multi-frequency viscoelastic data collected at a various temperature can be shifted along the frequency axis to a reference curve, thus a master curve is constructed. The distances between the curves give the values of shift factor (log a_T), which in some extent can reflect the rate of relaxation. In this work, three groups of log a_T values obtained by shifting storage modulus curves, loss modulus curves and tan δ curves along the frequency axis taking 256 K as reference temperature are plotted against temperature, as depicted in Fig. 5. The resulting master curves of storage modulus, loss modulus and tan δ are shown in Fig. 6. It is obvious that the TTS process is successful in the whole frequency range and the three groups of

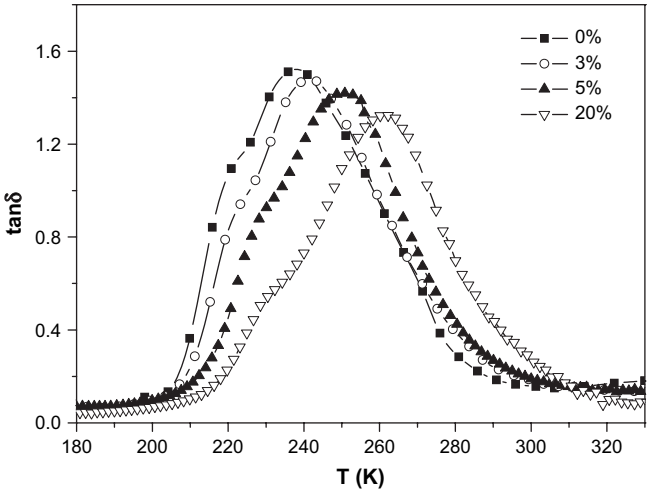

Fig. 4. The influence of the content of PR 201 on the tan δ peak of CIIR.

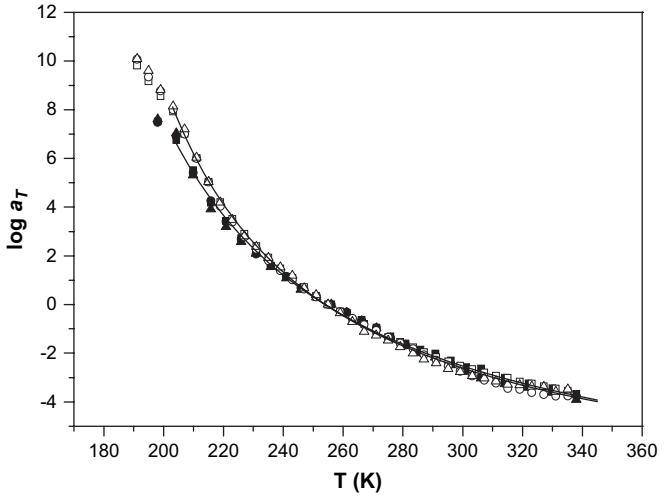

Fig. 5. Temperature dependence of log a_T of uncured (filled symbols) and lightly cured (open symbols) CIIR. The rectangles, circles and triangles represent log a_T values obtained from shifting storage modulus curves, loss modulus curves and tan δ curves, respectively. The lines are used to fit these data by VFTH equation.

shift factors almost overlap with each other. The master curve of tan δ also displays a two-peak structure with the shoulder peak on the higher frequency side and the maximum one on the lower frequency side. Fig. 6(a) additionally shows the frequency dependence of ε'' measured at 256 K. Again the ε'' peak corresponds to the high-frequency shoulder peak of tan δ master curve, suggesting its mechanism of local segmental motion.

It is found that the log a_T curves of both uncured and lightly cured CIIRs above 203 K can be described by Vogel–Fulcher–Tammann–Hesse (VFTH) equation:

$$\log\ a_T = A + B/(T - T_v) \tag{1}$$

where A, B and T_v are constants. The fitting process generates $A = -8.962$, $B = 1049$ and $T_v = 136.9$ for uncured CIIR, while $A = -8.598$, $B = 903.8$ and $T_v = 148.9$ for lightly cured CIIR. From, the temperature dependence of log a_T, the fragility of uncured and lightly cured CIIRs can be determined by [25] the following equation:

$$m = \mathrm{d}\ \log\ a_T/\mathrm{d}(T_g/T) \quad \text{or} \quad m = \frac{B/T_g}{\left(1 - T_v/T_g\right)^2} \tag{2}$$

here T_g is determined to be 203 K for both uncured and lightly cured CIIRs by PALS as mention in the following part of the paper. Consequently, the m value for uncured CIIR is 48.7, which is very close to $m = 46$ of PIB [26], suggesting that CIIR is a strong glass-forming liquid. This is consistent with Ngai's opinion that glass-forming liquids with low coupling parameter tend to have small fragility [27,28]. While for lightly cured CIIR, the m value is equal to 62.7. Hence, lightly cured CIIR is still a relatively strong glass-forming liquid but vulcanization increases its fragility. In Fig. 5, it is found that at the high-temperature side the log a_T values of lightly cured CIIR are nearly the same as these of uncured CIIR, but after

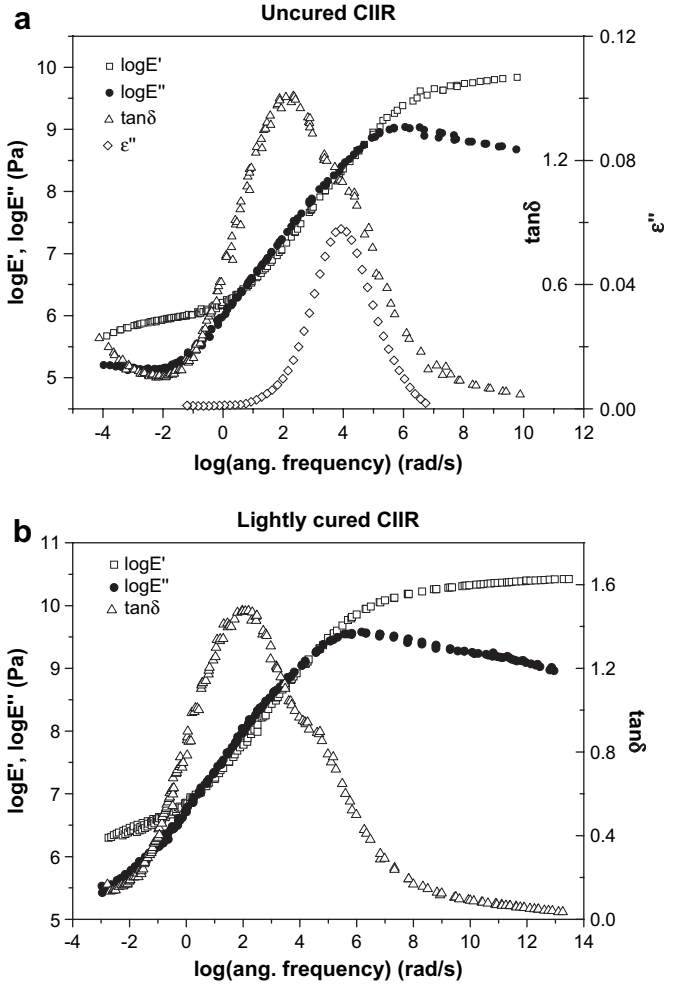

Fig. 6. The master curves of E', E'' and tan δ obtained from TTS analysis of DMA results taking 256 K as reference temperature. The frequency dependence of dielectric loss is also shown for uncured CIIR.

240 K gradual departure between them can be observed. Consequently, near the glass transition temperature, $\log a_T$ of lightly cured CIIR shows stronger temperature dependence, this corresponds to its increase of fragility. The phenomenon of crosslinking leads to the increase of fragility was also reported in several previous works [29,30]. It is pointed out that strong liquids are usually those with self-reinforcing tetrahedral network, stable structures and local to intermediate range order, and their properties do not change dramatically with temperature [31]. This is the reason why CIIR has a broad transition region.

DMA is a macroscopic measurement of the mechanical response of materials, so the above statements hereto require to be studied from atom scale. In order to understand the microscopic characteristics, PALS was previously used to study the dimension and content of free volume of CIIR [24]. In the present paper, a further insight into the results of PALS is given in the following discussion.

It is well known that the probability of *o*-Ps pick-off annihilation process is directly related to the electron density of the cavity wall and inversely associated with the free-volume hole radius, so the variation of the *o*-Ps lifetime with temperature directly reflects the thermal expansion of free-volume holes. Fig. 7 shows the *o*-Ps lifetime spectra of lightly cured and uncured CIIRs. The two spectra show the same tendency with the slope $d\tau_3/dT$ varying greatly in different temperature regions. Both curves clearly show two inflection points around 203 K and 270 K. The former is identified as T_g of CIIR, while the latter may arises from the slow process. In the process the thermal motion of longer chain segments weakens the interaction of molecular chains, which leads to faster expansion of free-volume holes after the slow process. From Fig. 7, it can be seen that τ_3 values of uncured and lightly cured CIIRs at T_g are about 1.23 and 1.29, respectively, which are relatively small values compared with other amorphous polymers [32], indicating that CIIR exhibits very effective chain packing. It has been reported that smaller τ_3 value at T_g corresponds to smaller fragility [32]. Therefore, being consistent with the results of DMA, PALS measurement also shows that CIIR is a glass-forming liquid with minimal fragility. Another phenomenon which should be noted is that the τ_3 rises quite slowly within the temperature range of 203 K and 270 K. Intuitively, the motion of longer chain segments needs larger space, while the effective chain packing and slow expansion process of free-volume holes does not afford such a condition, which inevitably retards the motion of longer chain segments. By contrast, the local segmental motion is little affected. As a result, the motion of longer chain segments and the motion of local segments separate from each other in time or temperature scale. This phenomenon may be another important reason for the two-peak structure, besides the low intermolecular co-operativity [7].

The *o*-Ps intensity (I_3), which reflects the change of free-volume concentration with temperature, is demonstrated in Fig. 8. It can be observed that I_3 of uncured CIIR shows the same trend as that of lightly cured CIIR. I_3 of both spectra reduces when temperature rises from 183 K up to 213 K and then increases. Thereafter, for lightly cured CIIR, from 233 K to 253 K, I_3 goes down again followed by a rising after 253 K; for uncured CIIR, the valley is not so obvious but

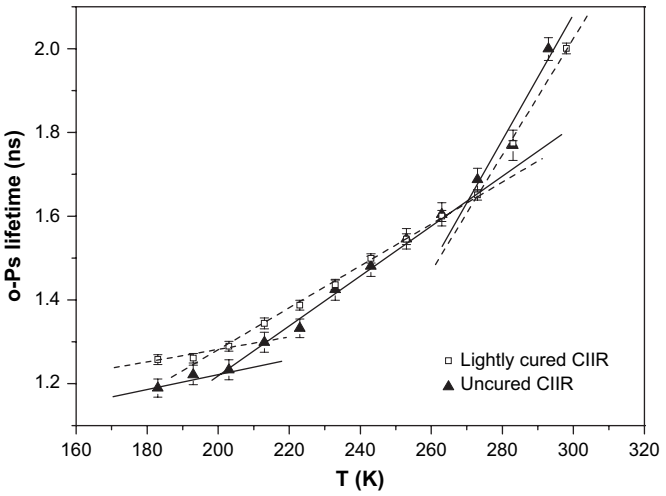

Fig. 7. Temperature dependence of *o*-Ps lifetime. The lines are used to guide the eyes.

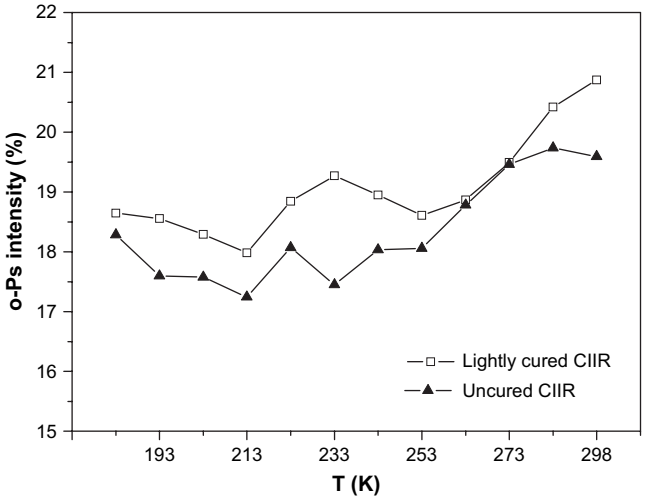

Fig. 8. Temperature dependence of *o*-Ps intensity. Since the absolute value of *o*-Ps intensity is not our concern, one of the curves is shifted along the *y*-axis to show more clearly.

a minimum I_3 value at 233 K can be observed. The change in I_3 implies some rearrangement of molecular chains, which finally causes some macroscopic effects, i.e., transitions. Therefore, the concentration fluctuations in I_3 may be corresponds to the α process and the slow process. But the exact mechanism leading to the concentration fluctuations is still unclear and needs further study. We propose a possibility that such a phenomenon of decrease in I_3 at the transition regions is probably a sign of molecular co-operativity. At the glass transition region, due to the effective chain packing of CIIR, the molecular chains are over crowded. Consequently, when chain segments undergo a transition to new conformations, the motion of one segment needs the co-operative rearrangement of adjacent segments to form one larger hole in order to accommodate enough space for the segment. As a result, free volume holes between the rearranged units become too small to be detected. The decrease in I_3 at the glass transition region can be found in some other polymers (as shown in Table 1). It is interesting to note in Table 1 that the phenomenon tends to transpire in nonpolar polyolefins and their derivatives, the majority of which are semicrystalline polymers. In these semicrystalline polymers, most of their molecular chains are smooth, symmetric and flexible, which is in favor of effective packing, furthermore, the amorphous molecular chains near the crystallites tend to be more closely packed. Hence I_3 fluctuation may also be expected in these polymers.

Table 1
Some polymers exhibiting a decrease in I_3 at the transition region

Polymer	Code	Reference
Polybutadiene	PBD	[33,34]
Polypropylene	PP	[34–36]
Polyethylene	PE	[35,38,41]
Ethylene/1-octene copolymers	P(E-*co*-O)	[37]
Ethylene-methylmethacrylate (3%) random copolymer	EMMA	[41]
Poly(silylenemethylene)s	PSM	[38]
Styrene–butadiene rubber	SBR	[39]
Poly(ethylene oxide-*co*-propylene oxide)	[P(EO/PO)]	[40]
Poly[ethylene oxide-*co*-2-(2-methoxyethoxy) ethyl glycidyl ether]	[P(EO/MEEGE)]	[40]

4. Conclusion

The molecular mobility through the glass transition of CIIR has been explored by DMA, DS and PALS. Both DMA and PALS results indicate two processes in CIIR: the low-temperature process is ascribed to the α process, while the high-temperature process is assigned to the slow process. The DS only detected the α process, which exactly corresponds to the shoulder peak in the loss tangent curve and can be definitely attributed to the local segmental motion. The slow process arises from the motion of longer chain segments, which may involve from decades to two or three hundreds of backbone bonds. The slow process exhibits stronger frequency dependence than the α process. DMA and PALS results also suggest that CIIR is strong glass-forming liquid, but vulcanization increases its fragility. It is further found from the temperature dependence of τ_3 value that CIIR exhibits very effective chain packing, which retards the motion of longer chain segments.

Acknowledgments

This work was financially supported by the National Natural Science Foundation of China (Grant No. 10276025) and the Ministry of Education (the Foundation for Ph.D. training, Grant No. 20040610027) of China.

References

[1] Plazek DJ, Chay IC, Ngai KL, Roland CM. Macromolecules 1995;28:6432.
[2] Fitzgerald ER, Grandine LD, Ferry JD. J Appl Phys 1953;24:650.
[3] Donth E, Berner M, Reissig S, Korus J, Garwe F, Vieweg S, et al. Macromolecules 1996;29:6589.
[4] Huang GS, He XR, Wu JR, Pan QY, Zheng J, Hong Z. J Appl Polym Sci 2006;102:3127.
[5] Sanders JF, Ferry JD. Macromolecules 1974;7:681.
[6] Boyer RF. J Appl Polym Sci 1986;32:4075;
Boyer RF. J Macromol Sci Phys 1980;B18:461.
[7] Stantangelo PG, Ngai KL, Roland CM. Macromolecules 1993;26:2682.
[8] Tanaka A, Ishida Y. J Polym Sci Part B Polym Phys 1974;12:1283.
[9] Richter D, Arbe A, Colmenero J, Monkenbusch M, Farago B, Faust R. Macromolecules 1998;31:1133.
[10] Krygier E, Lin GX, Mendes J, Mukandela G, Azar D, Jone AA, et al. Macromolecules 2005;38:7721.
[11] Capps RN, Burns J. J Non-Cryst Solids 1991;131:877.
[12] Sridhar V, Chaudhary RNP, Tripathy1 DK. J Appl Polym Sci 2006;100:3161.
[13] Kirkegaard P, Eldrup M, Mogensen OE, Peterson NJ. Comput Phys Commun 1981;23:307.
[14] Stockmayer WH. Pure Appl Chem 1967;15:539.
[15] Watanabe H. Macromol Rapid Commun 2001;22:127.
[16] Höfl S, Kremer F, Spiess HW, Wilhelm M, Kahle S, Kahlea S. Polymer 2006;47:7282.
[17] Sakamoto A, Ogata D, Shikata T, Urakawa O, Hanabusa K. Polymer 2006;47:956.
[18] Hirose Y, Adachi K. Polymer 2005;46:1913.
[19] Orbon SJ, Plazek DJ. J Polym Sci Part B Polym Phys 1985;23:41.
[20] Chen J, Kow C, Fetters LJ, Plazek DJ. J Polym Sci Part B Polym Phys 1985;23:13.

[21] Loomis LD, Zoller P. J Polym Sci Part B Polym Phys 1983;21:241.
[22] Chen J, Kow C, Fetters LJ. J Polym Sci Part B Polym Phys 1982;20:1565.
[23] Obon SJ, Plazek DJ. J Polym Sci Part B Polym Phys 1982;20:1575.
[24] Wu JR, Huang GS, Pan QY, Qu LL, Zhu YC, Wang B. Appl Phys Lett 2006;89:121904.
[25] Angell CA. J Non-Cryst Solids 1991;13:131.
[26] Huang DH, McKenna GB. J Chem Phys 2001;114:5621.
[27] Ngai KL, Gopalakrishnan TR, Beiner M. Polymer 2006;47:7222.
[28] Ngai KL, Roland CM. Macromolecules 1993;26:6824.
[29] Alves NM, Gómez Ribelles JL, Mano JF. Polymer 2005;46:491.
[30] Qazvini NT, Mohammadi N. Polymer 2005;46:9088.
[31] Debenedetti PG, Stillinger FH. Nature 2001;410:259.
[32] Bartoš J, Krištiak J. J Non-Cryst Solids 1998;235–237:293.
[33] Bartoš J, Šauša O, Bandzuch P, Zrubcová J, Kristiak J. J Non-Cryst Solids 2002;417:307.
[34] Wang CL, Wang SJ. Phys Rev B 1995;51:8110.
[35] Uedono A, Kawano T, Tanigawa S, Ban M, Kyoto M, Uozumi T. J Polym Sci Part B Polym Phys 1997;35:1601.
[36] Djourelov N, Suzuki T, Shantarovich VP, Dobreva T, Ito Y. Rad Phys Chem 2005;72:13.
[37] Kilburn D, Bamford D, Lüpke T, Dlubek G, Menkeb TJ, Alam MA. Polymer 2002;43:6973.
[38] Ogawa T, Suzuki T, Murakami M. J Polym Sci Part B Polym Phys 1998; 36:755.
[39] Wang JY, Vincent J, Quarles CA. Nucl Instrum Methods Phys Res B 2005;241:271.
[40] Uedono A, Tanigawa S, Watanabe M, Nishimoto A. J Polym Sci Part B Polym Phys 1998;36:1919.
[41] He CQ, Suzuki T, Ma L, Matsuo M, Shantarovichc VP, Kondo K, et al. Phys Lett A 2002;304:49.